Nonlinear electrohydrodynamic phenomena and droplet generation in charged jets of conducting liquid

V. N. Gorshkov and M. G. Chaban

Institute of Physics, Academy of Sciences of Ukraine, 252650 Kiev, Ukraine
(Submitted June 4, 1998; resubmitted October 23, 1998)
Zh. Tekh. Fiz. **69**, 1–9 (November 1999)

Phenomena occurring at the tip of a charged conducting jet are analyzed in detail using numerical methods developed for axially symmetric flows. Universal mechanisms (independent of the method for producing the jet) for droplet formation with different ratios of the Laplace and electrical pressures on the lateral surface are identified. An explanatory analysis is given for all of the nonlinear stages of the classical Rayleigh instability of a charged conducting drop, beginning with the formation of a jet at the surface of the drop and culminating in the generation of a developed jet of secondary droplets. © *1999 American Institute of Physics.* [S1063-7842(99)00111-7]

1. Studies of the physical mechanisms governing the breakup of a cylindrical liquid jet into droplets have a rather long history, beginning with the classical work of Rayleigh.[1] The ideas behind the linear theory of the instability of an infinite jet in the absence of an electric field are perfectly clear. Random small perturbations in its radius of the form $\varepsilon \exp(ikz)$ $(k=2\pi/\lambda)$ disturb the uniformity of the Laplace pressure $p_L=\alpha(1/R_1+1/R_2)$ at the surface (α is the coefficient of surface tension and $R_{1,2}$ are the principal radii of curvature). In the case of long-wavelength disturbances, p_L is determined by the curvature of the surface, $1/R_1$, in the plane perpendicular to the axis of the jet, and the liquid flows from constricted zones toward wider zones, which causes an exponential growth in the initial perturbations. For short-wavelength disturbances ($\lambda<\lambda_k=2\pi r_0$, where r_0 is the initial radius of the jet), the curvature $(1/R_2)$ of a surface passing through the axis ($R_2<0$ in a constricted region) becomes important. The resulting pressure imbalance leads to a reverse flow of liquid, to a reduction in the initial perturbations, and to surface oscillations. With increasing λ ($\lambda>\lambda_k$) the amplitude of the variations in $p_L(z)$ ($\Delta p_L \to 2\alpha\varepsilon/r_0^2$) increases, but at the same time there is an increase in the mass of liquid whose flow over a length equal to λ brings about the aperiodic development of each of the constrictions. The optimum value of λ, corresponding to the maximum growth rate, is given by $\lambda_m \approx 9r_0$.

If a conducting jet is charged, then λ_k and λ_m are smaller, since the negative electrostatic pressure, which is greater in absolute magnitude in regions with a high surface curvature, provides correctives to the pressure drop.[2]

As to the nonlinear stages of the development of the instability, for a long time little was known about the mechanism for droplet and satellite formation, when a jet breaks up at two cross sections to the right and left of the site of the original constriction, rather than at the constriction itself, thereby creating primary droplets with radii on the order of $1.9r_0$, as well as small droplets of size $r_0/3$ (for $\lambda=\lambda_m$).[3] Only a detailed analysis of a numerical simulation revealed the physical nature of this phenomenon.[4]

In technical applications droplets are generated by finite liquid jets. Thus the theoretical analysis of the instability of infinite jets is unsuitable for understanding the droplet formation process and choosing optimal operating conditions for the relevant devices. For example, the dynamics of extended liquid jets bounded on two sides (in the absence of an electric field) is beautiful and unexpected[5] from the standpoint of Rayleigh's classical approach.[1] In a contracting jet, periodic structures with a characteristic size of the order of $2r_0<\lambda_k$ are self-excited! During their capricious evolution, these jets create a series of droplets of different sizes. Breakup of this sort has been examined numerically in a number of papers[6,7] without analyzing the physical mechanisms for the phenomenon. One such analysis has been carried out[8] and it was shown that nonlinear surface waves are excited under the influence of an overpressure $p_L \approx 2\alpha/r_0$ at the ends of the jet (in the main region, $p_L \approx \alpha/r_0$). The peculiar ''resonance'' at a length λ_r of the order of $2r_0$ occurs because local perturbations in the surface pressure are transmitted by the liquid in both directions from the excitation zone with a characteristic damping length $\approx r_0$. The interaction of the counterpropagating waves leads to chaotic fractionation of the corrugated jet into droplets.

This phenomenon necessitates a new way of looking at the development of the Rayleigh instability of a jet flowing out of an orifice (of course, without contradicting the quantitative results of our predecessors). When there are no external interactions, it is customary to assume that the source of the initial perturbations is the thermal noise of the jet radius,[2] of which the harmonic with the highest growth rate γ_m is selected during transport along the flow. We regard this approach as incorrect and offer the following description of the process of droplet formation. The end of the jet, with a Laplace overpressure p_L, excites a corrugation in the surface with a period of $\lambda_r \approx 2r_0$. Nonlinear effects[8] subsequently give rise to the formation of a droplet at the end of

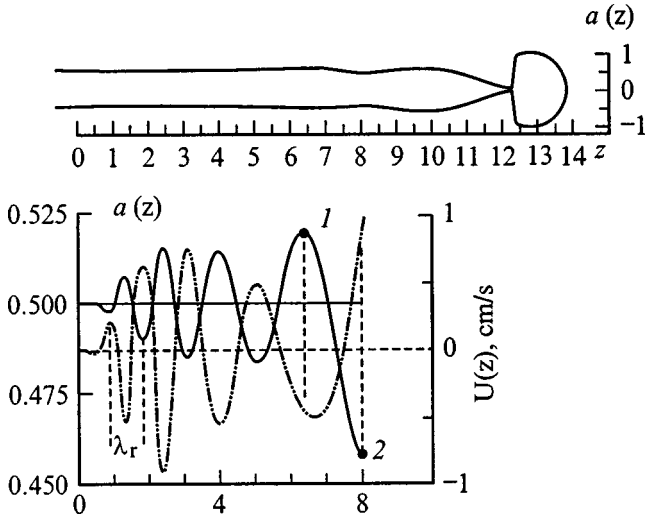

FIG. 1. Generation of droplets from a bounded jet of liquid (in the absence of external perturbations) owing to self-excitation of short-wavelength structures on the surface. Shown here are the full profile $a(z)$ of the perturbed portion of the jet (top) and fragments of the jet radius ($a(z=0)=0.5$ cm) and longitudinal velocity U of the liquid as functions of distance (bottom).

the jet, and a train of waves with the leading (shortest, in accordance with the dispersion relation of Ref. 1) ''resonant'' harmonic $\lambda_r \approx 2r_0$ (Fig. 1) propagates toward the base of the jet. The long-wavelength components that close the wave train impart to the surface a higher level of disturbances, not comparable to the thermal noise. The data of Fig. 1 were obtained from a numerical simulation according to the scheme of Ref. 8 for the dynamics of a cylindrical jet of water, bounded on the right, with a radius $r_0=0.5$ cm (neglecting the force of gravity and with zero initial liquid velocity). The time at which the third droplet breaks away is shown here. At the front of the train, the phases of the oscillations in the radius $a(z,t)$ of the surface and of the average longitudinal velocity $U(z,t)$ are shifted by π, which is typical of a wave process. The change in the phase shift at points *1* and *2* corresponds to growth of the perturbations ($\partial U/\partial z < 0$ at *1* and greater than zero at *2*). The waves are driven on account of the drop in surface energy during the formation of the next droplet. The process has not gone to completion, but the size of the droplet is already close to the observed value $\approx 1.9r_0$. It is difficult to escape the illusion that some perturbations are amplified as they are carried away from the base of the jet. In the steady state the time t_k for the jet to break up (droplets to form) can be estimated by equating the length of the cut-off portion of the jet, λ_m, to the distance the ''resonant'' harmonic propagates over the time t_k, i.e., by setting $\lambda_m = t_k V_{\rm ph}$, where $V_{\rm ph}$ is the corresponding phase velocity of the surface wave. After some calculations using the Rayleigh dispersion relation,[1] we obtain the standard formula $t_k \sim 2/\gamma_m$, in accordance with numerous experimental measurements.

These results will help later in interpreting the physical phenomena observed in our numerical simulations of the breakup of a charged conducting jet. Attempts to model the dynamics of conducting liquids in strong electric fields have been made previously, but the calculations ended at the stage when conical protrusions (Taylor cones) develop.[9,10] Jet regimes were simply unattainable with the numerical schemes employed there.

Based on general physical considerations, we can state that after a jet is formed, the electrohydrodynamic processes near its tip are independent of the manner in which it was produced. In our work we have chosen the instability of highly charged particles as a starting point. At some level of charge, known as the Rayleigh critical charge,[11] a drop becomes unstable and is deformed, ejecting a jet at whose tip droplets are generated. While there has been much theoretical and experimental work on the Rayleigh limit,[12] almost nothing is known about the dynamics of the breakup of a charged drop. Theoretical study of this phenomenon is made difficult by the strong nonlinearity of the process. The energy approach[13] to the problem cannot be used to determine the mechanisms for interesting nonlinear processes. The transient nature of jet breakup in various physical systems (liquid metal ion sources, electrospray devices[14,15]) and the small sizes of these jets make experimental investigation of the essence of many of these processes difficult. Even those phenomena which are detected experimentally are often associated with uncontrollable external interactions. For example, the generation of oblate (along the direction of an external electric field) spheroids, which, in turn, ejected new jets in a transverse direction, has been observed.[16] Far from the tip of the jet, prolate spheroids were observed, along with the generation of secondary droplets in the longitudinal direction. We have shown, in particular, that these are fragments of a single prolonged process, and not the result of aerodynamic effects.[16] The formation of a stepped (with thickening in the transition zone) jet profile (see the plots of $a(z,t)$ in Figs. 4–6) in the experiments of Taylor[17] is a regular stage in the evolution of the balance between the electrical and Laplace pressures along a jet as it grows.

2. For axially symmetric flows of a viscous, incompressible liquid with a free boundary we have used a model that we developed earlier.[8] This model provides a fairly accurate description of the dynamics of even relatively short-wavelength perturbations of the jet, although the longitudinal velocity of the liquid particles, $U(z,r,t)$, was assumed independent of the distance r to the axis. In this case, the radial velocity profile $V(r,z,t)$ is a linear function of r ($V(r,z,t) = V_0(z,t)r/a(z,t)$, where $V_0(z,t)=V(r=a,z,t)=da(z,t)/dt$ is the distribution of the radial component of the velocity of the points on the surface and $a(z,t)$ is the jet profile.), while the corresponding Navier–Stokes equation of motion in a cylindrical coordinate system takes the form

$$(\rho r/a)dV_0/dt = -\partial p_f/\partial r + \mu r \partial^2(V_0/a)/\partial z^2, \qquad (1)$$

where ρ and μ are the density and viscosity of the liquid.

According to Eq. (1), the spatial variation of the pressure $p_f(z,r,t)$ in the liquid is given by

$$p_f(z,r,t) = p_0(z,t) - (\rho r^2/(2a))dV_0/dt + (\mu r^2/2)\partial^2(V_0/a)/\partial z^2, \qquad (2)$$

where $p_0(z,t)$ is the pressure on the jet axis.

Since the pressure p_f at $r=a$ in a given transverse cross section of the jet equals the surface pressure $p_S(z,t)$, we obtain the following equation for the velocity $V_0(z,t)$ from Eq. (2):

$$\rho dV_0(z,t)/dt = 4[p(z,t)-p_S(z,t)]/a(z,t) + \mu a\partial^2(V_0/a)/\partial z^2, \quad (3)$$

where $p(z,t)=(p_0(z,t)+p_S(z,t))/2$.

The force F_z acting on a transverse cross section of the jet is determined by integrating Eq. (2) from 0 to a. Making some transformations using Eq. (3), we obtain $F_z = \pi a^2(z,t)p(z,t)$. Our earlier assumption that $\partial U(z,r,t)/\partial r=0$ signifies an arbitrary division of the liquid into thin disks (truncated cones) whose boundaries have velocities $U(z,t)$. Including all the forces acting on a disk of this sort with thickness Δz leads to an equation for the longitudinal velocity $U(z,t)$,

$$\rho dU(z,t)/dt = -\partial p/\partial z + \mu\partial^2 U(z,t)/\partial z^2 + 2[p_S-p]\partial(\ln a)/\partial z. \quad (4)$$

The right-hand side of Eq. (4) includes terms owing to the gradient in F_z and to the surface force $2\pi a p_S(z,t)\Delta z\partial a/\partial z$ acting on the lateral surface of the disk in the longitudinal direction. Thus Eq. (4) is the standard Navier-Stokes equation of motion including the existence of a free boundary for the given macroscopic particle.

The equation for $p(z,t)$ is easily obtained as follows. We select a jet segment of length Δz and radius $a(z,t)$. When it is deformed during the flow, $a^2(z,t)\Delta z(t)=\text{const}$. Differentiating this equation with respect to time yields

$$2\Delta z(t)da(z,t)/dt + a(z,t)d(\Delta z(t))/dt = 0. \quad (5)$$

Since $d(\Delta z(t))/dt = \Delta z(\partial U/\partial z)$, Eq. (5) yields the equation of continuity for the flow,

$$2V_0(z,t)/a(z,t) + \partial U(z,t)/\partial z = 0. \quad (6)$$

Again, differentiating Eq. (5) with respect to time and using Eq. (6) and the equation $d^2(\Delta z(t))/dt^2 = \Delta z[\partial(dU/dt)/\partial z]$ yield

$$dV_0/dt = 3V_0^2/a + (a/2)[\partial(dU/dt)/\partial z]. \quad (7)$$

After substituting the right-hand sides of Eqs. (3) and (4) in Eq. (7), we obtain a rather cumbersome equation for $p(z,t)$, for which a satisfactory difference approximation that conserves the total volume of liquid is far from obvious. However, such a computational scheme is easily constructed without direct recourse to Eq. (7). (A detailed description of this method is given in Ref. 8.)

The approximation $\partial U(z,r,t)/\partial r=0$ has been used in many papers. It limits the use of the initial system of equations for numerical study of short-wavelength perturbations of a jet. In our work, however, this was the only approximation. In the following we calculate the internal pressure of the liquid and do not profile it in some way, as was done, for example, in Ref. 18: $p_f(z,r,t)=p_S(z,t)$ (after which the equation of motion was solved only for a single component of the velocity and the second component was determined from the equation of continuity). In accordance with Eqs. (2) and (3), we obtain a relationship between the local value of p_f and its average $p(z,t)$ over the transverse cross section of the jet in a natural way,

$$p_f(z,r,t) = p_S(z,t)(2(r/a)^2-1) + 2p(z,t)(1-(r/a)^2) \quad (8)$$

and the equations of motion for each component of the velocity, together with the equation for $p(z,t)$, are solved self-consistently, which ensures conservation of the volumes of each cell (macroscopic particle) of liquid during deformation (during the flow).

This approach extends the range of possibilities for the system of Eqs. (3) and (4) employed here. Thus the dispersion relation for small amplitude surface waves in infinite jets of radius r_0 obtained from the approximate system of hydrodynamic equations has no significant errors compared to an exact solution, even for wavelengths $\approx \pi r_0/2$.[8]

In the cases of low viscosity and slowly varying jet radius, $p(z,t)$ is determined by the steady state diffusion equation

$$\partial^2 p/\partial z^2 - (8/a^2)(p-p_S) + 6\rho(V_0/a)^2 = 0. \quad (9)$$

In our problem, the surface pressure $p_S(z,t)=p_L(z,t)-p_E(z,t)$, where $p_L=\alpha(1/R_1+1/R_2)$, $R_1=a\psi$, $R_2=-\psi^3(\partial^2 a/\partial z^2)^{-1}$, $\psi=[1+(\partial a/\partial z)^2]^{1/2}$, $p_E(z,t)=E^2(z,t)/8\pi$, and $E(z,t)$ is the electric field strength at the surface.

In the case of an ideally conducting liquid, the charge density distribution is found from the condition that the electrical potential be constant at all points on the surface.[19] The liquid was entirely broken up into a set of truncated cones (with a small ratio of the cone height to the radius of its average cross section) with their planes perpendicular to the axis of the flow. The charge densities σ_i on the lateral surface of each of these cones of area s_i are determined from the system of equations $\Sigma b_{ki}\sigma_i + \varphi_k = V(t)$ and $\Sigma S_i\sigma_i = Q$ if the flow dynamics is considered to have a specified charge Q ($V(t)$ is the surface potential and φ_k is the potential created by the external field on the surface of cone number k). In calculating the coefficients b_{ki}, the charge on the ith cone is usually represented by a system of point charges located on the middle line of the side surface of the cone, which simplifies the averaging procedure. In our case, where we are solving the stability problem and highly accurate field calculations are necessary, this approximation is unsuitable (especially for calculating the diagonal elements b_{kk}). In the exact expression for b_{ki} an analytic integral is taken with respect to z and a partially numerical and partially analytic integral with respect to the azimuth. This computational method ensured a relative error in the determination of the charge density of less than 0.01% compared to the known analytic solutions. We supplement Eqs. (1)–(3) with the initial and boundary conditions. At $t=0$ a droplet of radius r_0 with its center at the coordinate origin $r=0$, $z=0$ is deformed into an ellipsoid of revolution that is prolate along the Z axis with semiaxes $r_0(1+\delta)$ and $r_0(1+\delta)^{-1/2}$, where $\delta=0.05$. The initial velocities $U(z,t=0)=V_0(z,t=0)=0$ and the total electric charge on the surface equals Q. The boundary conditions are

$$\partial V_0/\partial z|_{z=0} = \partial p/\partial z|_{z=0} = U(z=0,t) = 0,$$

$$a(z_c,t) = 0, \quad p(z_c,t) = p_S(z_c,t), \tag{10}$$

where $z_c(t)$ is the coordinate of the end of the jet.

At each time step the electrostatic problem was solved to determine $p_E(z)$ and $p_L(z)$ was calculated for the given $a(z)$. Then the function $p(z)$,[8] was determined using Eqs. (3), (4), (7), and (10). After that, the new velocities and coordinates $a(z,t+\Delta t)$ were determined using the same Eqs. (3) and (4). As the droplet deforms, the coordinate grid is periodically realigned to ensure the required accuracy of the model for the jet formation and dynamics.

Note that the numerical model for the hydrodynamic part of the problem comes well recommended for studies of the dynamics of self-excited short-wavelength periodic structures in bounded jets.[8] When we included the electrostatic part, as a test we calculated the small oscillations of a droplet with a subcritical charge. The resulting agreement with the analytic solution[11] for the period of the oscillations offers the hope that the calculations will be reliable in more complicated cases.

For small deformations of the droplet, which are described using the associated Legendre polynomials, the first of the modes becomes unstable for $Q>Q_R=(16\pi\alpha r_0^3)^{1/2}$, the Rayleigh limit in the absence of an external electric field for $n=2$ in the dispersion relation[11]

$$\omega^2 = n(n-1)[(n+2)\alpha - Q^2/(4\pi r_0^3)]/(\rho r_0^3). \tag{11}$$

In our calculations we shall change the supercriticality parameter δ_e, defined by $Q=(1+\delta_e)Q_R$. For a given δ_e, the initial system of Eqs. (3), (4), and (6) is reduced to dimensionless form by introducing the new variables $t'=t(\alpha/(\rho r_0^3))^{1/2}$, $z'=z/r_0$, $a'=a/r_0$, and $\mu'=\mu/(\rho\alpha r_0)^{1/2}$. Thus, all of the many solutions of the problem are determined by two parameters: δ_e and μ'. For simplicity, we have assumed that $\rho=1$ g/cm^3, $r_0=0.5$ cm, and $\mu=1$ gs^{-1}cm^{-1}, and varied δ_e and α in the calculations.

3. Figure 2 shows the results of a numerical simulation with a fairly substantial excess charge on the droplet $Q_R(\delta_e=0.3,0.5)$. In this case the dimensions of the jet of secondary droplets are comparable to those of the initial drop, so it is easier to analyze the electromagnetic phenomena. In Fig. 2 and below, the pressure is given in g/(s^2 cm) and the velocity, in cm/s, while the profiles of the surfaces are given without distorting the ratio of the longitudinal and transverse dimensions. Two features of the process by which a drop breaks up can be seen easily in Fig. 2: (1) the region in which the jet develops (the distance from the minimum radial velocity to the end of the jet; curves *2–4* of Fig. 2a) narrows abruptly in time, and (2) the end of the jet is far from spherical in shape and its cutoff is accompanied by the formation of an oblate secondary droplet.

Equation (9) shows that the depth to which the negative overpressure penetrates into the depth of the liquid at the end of the jet (Fig. 2a, inset), where $p_S(z)>p_S(z_c)$ on the surface, is proportional to some effective value of a that depends on the shape of the surface near $z\sim z_c$. A narrowing of the jet with acceleration takes place only in the region

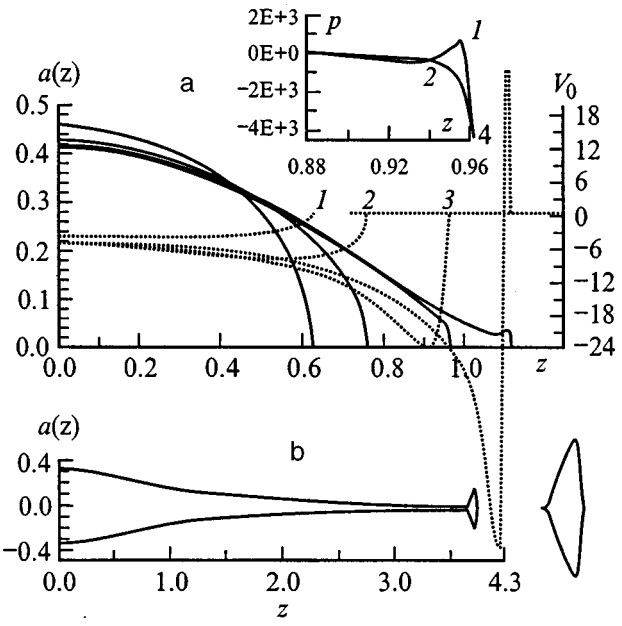

FIG. 2. a: Profiles of the droplet surface and the radial velocity (curves *1–4*) for $\delta_e=0.3$; $\alpha=300$ g/s^2; $t=0.0257$, 0.0319, 0.0354, 0.0363 s. Inset: *1* — $p_S(z)$, *2* — $p(z)$ at $t=0.0354$ s. b: $\delta_e=0.5$, $\alpha=75$ g/s^2. The initial droplet shape at the time the droplet/leader breaks away, $t=0.0799$ s. (A magnified view of the droplet is on the right.) Droplet radius for a spherical shape, $r_k=0.1$ cm, charge on the droplet $q_k=0.085Q$.

with $p(z)-p_S(z)<0$. Elongation (tapering) of the tip reduces the penetration depth of the increasing (in absolute value) $p_S(z_c)$. In addition, the negative pressure is squeezed out from the depth of the jet ($z<z_c$) toward its end by the pressure ''sources'' $\propto V_0^2/a^2$ in Eq. (9). As a result, the cutoff zone for the secondary droplet (the minimum in V_0) swiftly approaches the end of the jet, while the cutoff velocity increases sharply (Fig. 2a).

The formation of an oblate droplet seems strange only at first glance. But for a spherical or ellipsoidal (prolate) end of the jet, an even thinner jet would extend from its tip, and so on, until the size of the secondary droplets reached zero. On the other hand, for $Q>Q_R$ configurations in the form of an oblate ellipsoid of revolution are stable against small axially symmetric deformations.[20,21] Since any external fields will deform a spherical droplet into an prolate ellipsoid, under real conditions with $Q>Q_R$, according to Basaran's hypothesis,[21] oblate spheroids cannot be observed. However, as we shall see, during the breakup of a jet such configurations can develop naturally if the charge on the secondary droplet exceeds a critical value. Let us follow the dynamics of a jet after the lead droplet breaks away (Fig. 2b). The screening of the end of the jet by the charge of the first droplet causes the Laplace pressure p_L, which tends to shorten the jet, to dominate in this zone. Under these conditions, the already familiar mechanism exciting surface corrugation operates.[8] The region where the nucleus of the second droplet adjoins the main part of the jet ($R_2<0$) becomes a zone with a reduced pressure p_S (inset to Fig. 3). The flow of liquid into this zone from the jet leads to the development of a constriction[1)] (inset to Fig. 3) and to the simultaneous development, at its left, of a new region with an elevated pres-

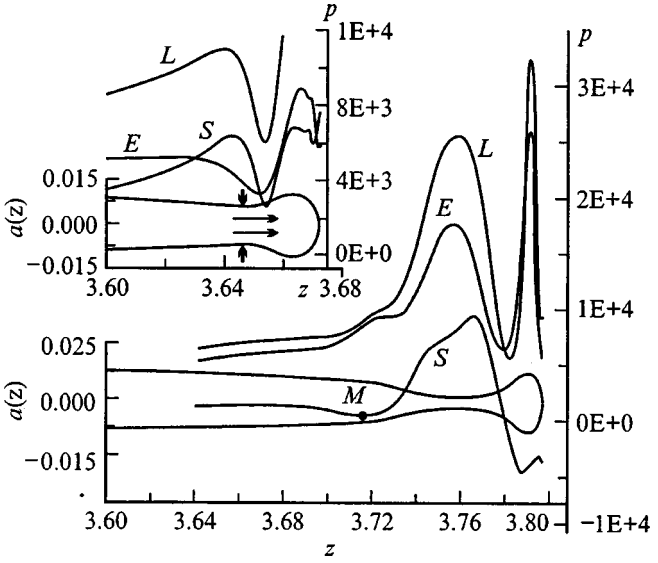

FIG. 3. Self-excitation of corrugation on the jet surface after breakaway of the droplet/leader (the continuation of the variant of Fig. 2b). Profiles of the surfaces and pressures $p_L(z)$, $p_E(z)$, and $p_S(z)$ (the corresponding subscripts are indicated beside the curves) for $t=0.0811$ and 0.0803 s (inset).

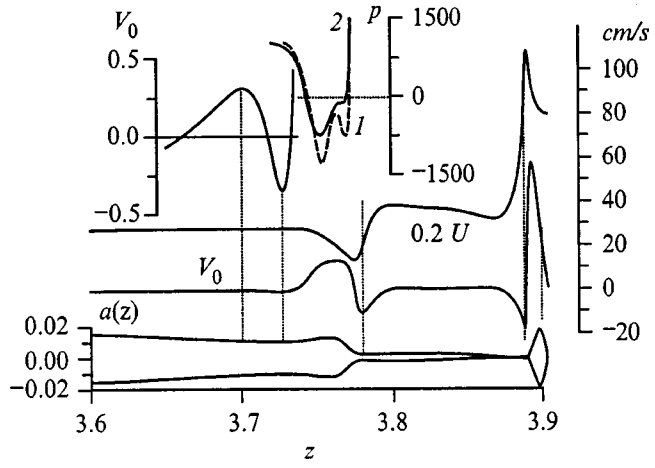

FIG. 4. Spatial variations in the characteristics of the jet (continuation of Fig. 3) at the time a second droplet breaks away: $t=0.0815$ s, $r_k=0.012$ cm, ratio of the charge q_k to the corresponding critical value q_R equals 1.277. The inset above shows fragments of $V_0(z)$, $p_S(z)$ (*1*) and $p(z)$ (*2*).

sure p_S (the next element of the corrugation or the next period of the surface wave) owing to the development of a curvature $1/R_2$.[8] If the charge on the surface were neglected, the process would proceed as shown above (Fig. 1). In this case (the lower part of Fig. 3), however, the screening of the tip of the jet (emitter) decreases as the lead droplet moves away, and this causes an influx of charge. The pressure $p_E(z_c)$ that draws out the jet increases. A second droplet rushes in behind the first and the electric field in the zone where the crest of the surface wave develops (in the future, the third droplet) increases so much as a result of the redistribution of the charge, that a minimum appears in the profile of the total pressure p_S (point M in Fig. 3). The influx of liquid into this zone rises and the amplitude of the crest increases. This leads to further charge accumulation and a negative pressure p_S (inset to Fig. 4). Thus the initial corrugation generated in the course of nonlinear wave processes transforms into an aperiodic instability regime.

As the jet evolves, the characteristic stepped surface profile, which is observed in experiments,[17] develops (Fig. 4). The necks joining the second and third droplets adjoin regions of reduced pressure p_S to their left and right. This situation ends, as is known,[8] in the breakup of the jet at two points (see the $V_0(z)$ profile in Fig. 4; $z_{1,2}\approx 3.78, 3.88$ cm) and the formation of a thin, elongated satellite. Naturally, it will also break up, in accordance with the above scenarios, and generate a multitude of microscopic droplets.

We did no further calculations of the process, but the formation of the next droplet is already noticeable in the radial velocity profile (inset to Fig. 4). The secondary droplets will approach a spherical shape as the residual charge on the initial droplet (the electric field at the tip of the emitter) decreases with time.

Droplet formation is, therefore, entirely determined by nonlinear electrohydrodynamic phenomena at the end of the jet. Previously formed, charged droplets affect the nucleation of new droplets through their electric fields. Thus we should expect some scatter in the sizes of the main droplets and the satellites. (Microscopic droplet chaos of this sort has been observed in liquid metal ion sources.[22])

In the version we examine here (Figs. 2–4), the relatively large δ_e and viscosity of the liquid (parameter μ') caused initial ejection of a jet whose size was such that, in its main part (outside the droplet formation region), the Laplace pressure exceeded the electrical pressure (Fig. 3). For small supercriticalities δ_e and large α (smaller μ'), a thinner jet develops, so that the ratio of p_L and p_E at its lateral surface changes: $p_L<p_E$. In this case, after part of the charge is ejected, we return to the previous (softer, so to say) droplet formation regime. But the initial stages of the breakup of the jet have a somewhat different mechanism for self-excitation of the corrugation in the surface (Fig. 5). Before discussing the physical bases of this phenomenon, let us make a simple mathematical analysis of the topological properties of the function $p_S(z)$ in that part of the liquid which can be called a jet. In the variant of Figs. 2b and 3, a function that rises on the left ($dp_L/dz>0$, since $dR_1/dz<0$) ends on the right with a region where it falls ($dp_S(z)/dz<0$), the electrical charge accumulates, and the electrical pressure dominates. In the intermediate region, $p_S(z)$ should have N maxima and $N-1$ minima. For $N=1$ (the ''fundamental'' mode), the highly charged tip of the jet with $p_S<0$ is cut off (for the profile of Fig. 2b, to the left of the droplet/leader $p_S>0$). The modes $N=2$ and above correspond to cutoff of the droplet with subsequent excitation of a surface wave (to the left of the cutoff zone) by the main pressure jump (inset to Fig. 3, $N=2$).

In the variant shown in Fig. 5 a fairly protracted zone develops in which $p_S(z)<0$. From the standpoint of topology, there is no prohibition on the formation of a pressure maximum $p_S(z)$ to the left of this zone. This sort of pressure jump actually does develop in the later stages of evolution of the jet and ''threatens'' to cut it off at the base as a whole. To generate droplets from the jet, itself, $\max p_S(z)$ must occur in the region where $dp_S(z)/dz<0$ at the left and right

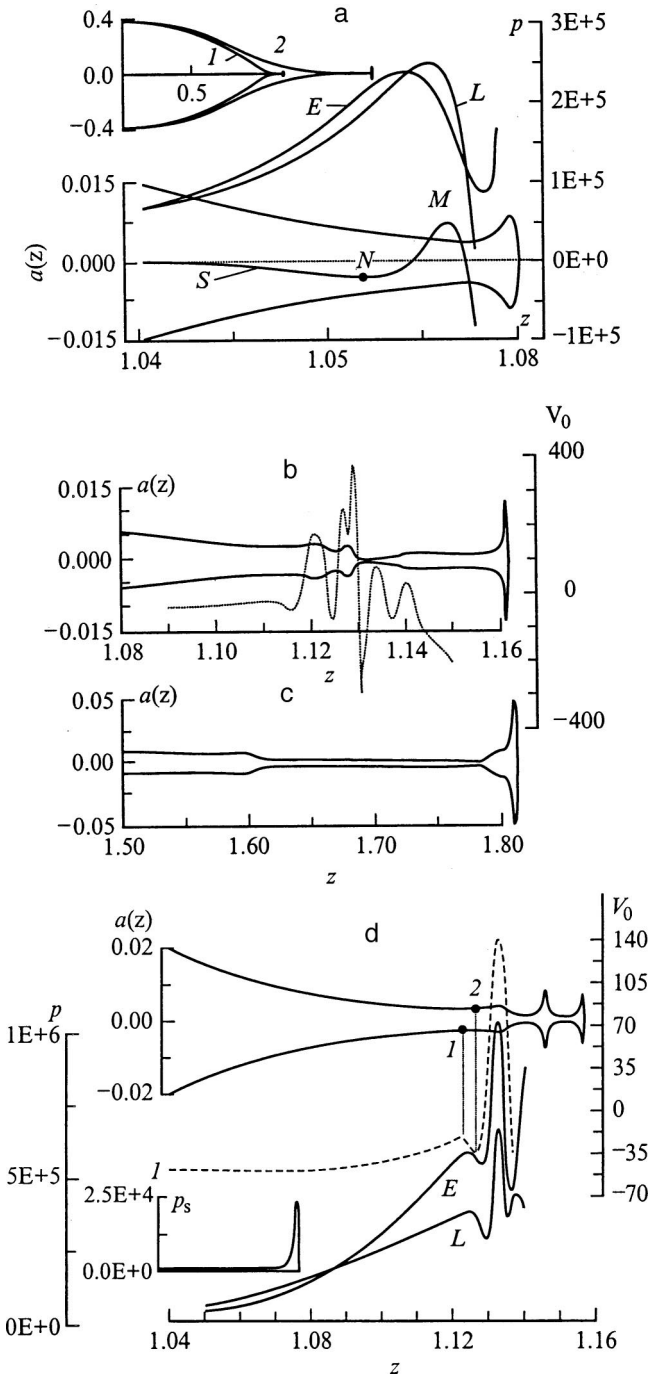

FIG. 5. Illustrating the mechanism for excitation of corrugation in the jet surface for small δ_e. a: — Profiles of the surface and pressures for $\delta_e = 0.05$, $\alpha = 1200$ g/s^2 at $t = 0.06177$ s (the inset shows the overall form of the $a(z)$ curves shown in Fig. 5b and 5c); b: continuation of Fig. 5a: $a(z)$, $V_0(z)$ (dotted curve) for $t = 0.06181$ s; c: $a(z, t = 0.1508\,\text{s})$, $\delta_e = 0.08$, $\alpha = 75$ g/s^2; d: continuation of the variant of Fig. 5b: profiles of the jet surface, $p_L(z)$, $p_E(z)$, and $V_0(z)$ (dotted curve) $\Delta t = 1.7 \times 10^{-5}$ s after breakaway of the head of the jet at the point $z = 1.13$ cm (Fig. 5b). The inset shows $p_S(z)$ within the interval [0;1.09].

ends. Under these conditions, however, extrema can develop only in pairs (max and min, Fig. 5a). Thus a constriction which cuts a droplet off from the tip of the jet (point M) is inevitably accompanied by a broadening of the flow channel (point N)– a prototype of the next (second) droplet. Physically, the extrema in the pressure $p_S(z)$ develop in the following way. If the values of p_L depend only on the local curvature of the $a(z)$ profile, then, besides this factor, the magnitude of the electric field is determined by the distribution of the charge over the entire surface of the deformed droplet. In Fig. 5a, the reduction in p_E on approaching the end of the jet (where a negative curvature $1/R_2$ appears) begins earlier than the reduction in the pressure p_L because of the screening effect of the charge at the tip, which is increasing with time. The shift in the peaks of p_E and p_L creates the two extrema in $p_S(z)$.

The lowered pressure $p_S(z)$ in the region of point N (like the Laplace overpressure in the variant examined before; Fig. 3) initiates self-excitation of corrugation in the surface in the direction of the base of the jet. The formation of a second drop causes electrical charge to accumulate on its surface and a zone with negative curvature $1/R_2$ to form to the left of it. Conditions for formation of a new pair of extrema in $p_S(z)$ are created, etc.

In a later stage of breakup, a distinctive surface profile is observed (Fig. 5b). In this experimental situation it is difficult not to attribute this profile to some uncontrolled perturbations, but, as we have seen, it is the natural evolution of a charged jet. If we increase the viscosity parameter μ', then with the same mechanism for the initial corrugation, the jet profile will be smoother (Fig. 5c).

Figure 5d shows the characteristics of the jet $\Delta t = 1.7 \times 10^{-5}$ s after it has broken off at the point $z = 1.13$ cm of Fig. 5b. Points 1 and 2 correspond to the fourth min and max pair in $p_S(z)$. The formation of the following constrictions and crests can be seen in the $V_0(z)$ profile. The ''principal'' maximum of the pressure $p_S(z)$ has formed near $z \approx 1.07$ cm (inset). This is a transition region between droplet and jet, where the liquid accelerates in the radial (toward the axis) and longitudinal directions before entering the jet. Subsequently, the loss of charge during generation of secondary droplets causes a reduction in the electrical pressure on the surface of the jet and a contraction of the zone where $p_S(z) < 0$. Droplet formation enters the regime shown in Figs. 2b, 3, and 4. In the concluding stage, the jet may be cut off as a whole in the transition region (a similar effect develops in Fig. 4, $z = 3.78$ cm).

If a constant potential is maintained on a jet, then after a large number of droplets have been generated in the interelectrode gap, the electric field on the jet will decrease owing to its being screened by secondary droplets. Periodic breakoff of the jet from the Taylor cone in liquid metal ion sources produces low frequency oscillations in the ion current.[22] As for the ion generation process in these devices, based on the results obtained here (Figs. 4 and 5), it is difficult to conceive that it can take place from a ''hemispherical tip,'' as assumed in a number of papers on the theory of these sources.[14,22]

The possible effect of an electric field on the coefficient of surface tension has been neglected in our calculations. In the most important region for droplet formation (Fig. 5d), $p_E > p_L$. Corrections to the Laplace pressure do not change the physical essence of these phenomena.

Any local pressure perturbations in the region where surface waves are excited (Figs. 3 and 5) will be damped over a

distance Δz from the localization region in proportion to $\exp(-3|\Delta z|/r_c)$ (r_c is the jet radius) according to Eq. (9); that is, they hardly exist for $\Delta z \approx \pm r_c$. During self-organization of the structure of the liquid flow and the surface pressure profile, elements with a characteristic size $\approx 2r_c$ appear, which have been broken off from the tip of the emitter by the strong electric field. Thus in the variants shown in Figs. 4 and 5d, the droplet radius r_k in the initial generation period is of the order of the jet radius ($r_k/r_0 \approx 2.4\times10^{-2}$ and 6×10^{-3}; $q_k/Q \approx 1/300$, $1/700$; $q_k/q_R \approx 1.3$ and 3, where q_R is the critical charge for a spherical droplet shape). As the electric field at the jet surface decreases, the scenario for droplet formation approaches the regime shown in Fig. 1 ($r_k \approx 1.8r_c$).

Let us note yet another feature of droplet formation. As we saw above, the secondary droplets are in the form of oblate spheroids with electrical charges above the critical level. These configurations are unstable with respect to small deformations into a triaxial ellipsoid.[23] Thus we present the scenario for the evolution of the secondary droplets as follows. Microscopic jets develop in the equatorial part of the oblate spheroids and new droplets are generated. This process is possible for the lead droplets in Figs. 4 and 5 until breakoff from the initial droplet. If, on the other hand, the excess charge is not too high (the instability growth rate is low), then breakup of the secondary droplets (with ejection of jets in a direction perpendicular to the direction of motion) will be observed near the tip of the initial jet. As the microscopic droplets are generated, the droplet charge falls below critical. The radial compression of the droplet owing to the Laplace pressure transforms it (because of inertia) into a prolate ellipsoid. Under these conditions, a third stage of jet formation is possible (in a zone further from the emitter), again in the longitudinal direction, even if $q_k < q_R$.[24] This type of dynamics for multistep droplet generation has been reported before, but the observed breakup of oblate and prolate ellipsoids was attributed to random aerodynamic effects.[16,25]

As an illustration of the third stage of droplet formation let us consider the breakup of an uncharged spherical droplet in an external electric field that is below critical $E = 0.9E_T$. (The critical field is[24] $E_T = 1.625(\alpha/r_0)^{1/2}$.) As it stretches out along the field, the droplet passes the equilibrium position as a result of inertia and is sufficiently deformed for instabilities to develop at its tips (Figs. 6a and b).

In Figs. 4, 5b, and 6b, characteristic $p_S(z)$ and $V_0(z)$ profiles with three extrema develop in the regions where the crest of the surface wave has developed ($p_S(z) < 0$, $V_0 > 0$). Figure 6c shows a typical structure of the spatial distributions of the electrical and Laplace pressures in this kind of zone. As the crest develops, $p_E(z)$ and $p_L(z)$ increase at its peak and decrease to the right and left because of the increasing negative curvature of the surface, $1/R_2$. As a result, the initial minimum in the total surface pressure p_S, which stimulates the development of the crest, splits into two minima. (See Fig. 6c; see also around point *M* in Fig. 3 and the inset with a fragment of $p_S(z)$ in Fig. 4.) Note that the increase in the Laplace pressure at the peak of the crest precedes the increase in the electrical pressure and limits the development of surface instabilities in the nonlinear stages. As these calculations show, even before they break away from the jet, the oblate spheroids formed at the tip of the emitter undergo small, axially symmetric (according to our model) oscillations about some equilibrium position.

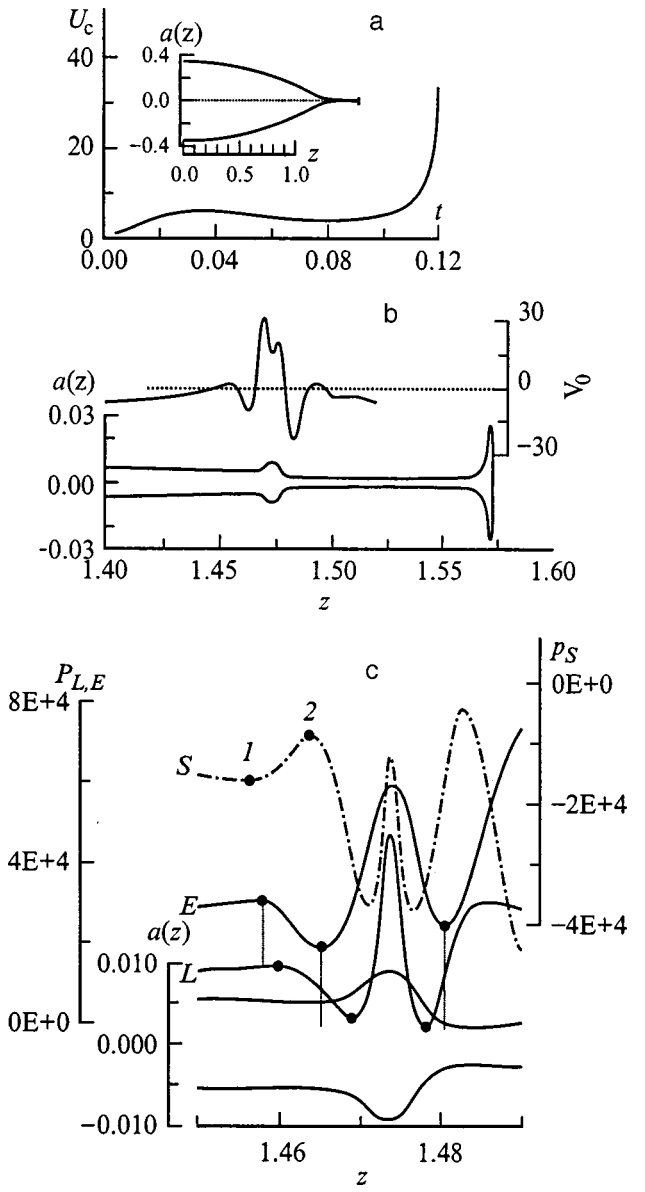

FIG. 6. Breakup of an uncharged droplet in an external electric field. $E = 0.9E_T$, $\alpha = 75$ g/s^2. a: Time dependence of the velocity of the jet tip $U_c = U(z_c, t)$; the inset shows $a(z, t = 0.1228\ \text{s})$; b: fragments of the surface profile and radial velocity near the tip at $t = 0.1228$ s; c: fragments of $p_L(z)$, $p_E(z)$, $p_S(z)$ and $a(z)$ in the region where the jet widens substantially ($t = 0.1228$ s). The extrema of $p_S(z)$, *1* and *2*, are the zones where constrictions on the jet surface and the subsequent crest of the wave develop (see the $V_0(z)$ profile in Fig. 6b).

Droplet generation from a jet of highly conducting, charged liquid is, therefore, determined by a complex of nonlinear electrohydrodynamic processes: excitation of nonlinear surface waves in relatively low electric fields at the tip of the emitter and of short-wavelength aperiodic instabilities with the formation of pairs of extrema in the total surface pressure in strong fields, formation of secondary droplets in the form of oblate ellipsoids, formation of extended satellites

(which break up into a series of microscopic droplets following the same scenario as for the main jet), and stepwise breakup of the secondary droplets through the generation of microscopic jets perpendicular and parallel to the direction of motion (the direction of the external electric field).

[1)]The development of a constriction under these conditions is an essentially nonlinear effect. According to the linear theory, for short-wavelength perturbations the surface pressure increases monotonically with z on going from the zone of the minimum jet radius as the jet expands, and a constriction cannot develop. However, because of nonlinear effects in the formation of the $p_L(z)$ profile, in our case the minimum p_S lies to the right of the constriction.

[1] Lord Rayleigh, Proc. London Math. Soc. **10**, 4 (1878).
[2] S. S. Nazin, A. N. Izotov, and V. B. Shikin, Dokl. Akad. Nauk SSSR **285**, 121 (1985) [Sov. Phys. Dokl. **30**, 606 (1985)].
[3] A. F. Ginevskiĭ and A. S. Dmitriev, in *Physicotechnical Problems in the Study of Monodisperse Systems*, Collected Scientific Papers, No.149 [in Russian], MÉI, Moscow (1987), pp. 5–24.
[4] V. V. Vladimirov and V. N. Gorshkov, Zh. Tekh. Fiz. **60**(11), 197 (1990) [Sov. Phys. Tech. Phys. **35**, 1349 (1990)].
[5] Ya. E. Geguzin, *Droplets* [in Russian], Nauka, Moscow (1977), 176 pp.
[6] N. Tjahjadi, H. A. Stone, and J. M. Ottino, J. Fluid Mech. **243**, 297 (1992).
[7] N. N. Mansour and T. S. Lungren, Phys. Fluids A 1990. **2**, 1141 (1990).
[8] V. N. Gorshkov and D. V. Mozyrskiĭ, Zh. Tekh. Fiz. **66**(10), 15 (1996) [Tech. Phys. **41**, 980 (1996)].
[9] C. Zheng and T. Linsu, J. Vac. Sci. Technol. B **6**, 2104 (1988).
[10] J. D. Sherwood, J. Fluid Mech. **188**, 133 (1988).
[11] Lord Rayleigh, Philos. Mag. **14**, 184 (1882).
[12] E. J. Davis and M. A. Bridges, J. Aerosol Sci. **25**, 1179 (1994).
[13] A. I. Grigor'ev and S. O. Shiryaeva, Zh. Tekh. Fiz. **61**(3), 19 (1991) [Sov. Phys. Tech. Phys. **36**, 258 (1991)].
[14] T. Hiramoto, K. Hirakawa, and Y. Ikoma, J. Vac. Sci. Technol. **6**, 1014 (1988).
[15] M. Cloupeau and B. Prunet-Foch, J. Aerosol Sci. **25**, 1021 (1994).
[16] A. Gomez and K. Tang, Phys. Fluids **6**, 404 (1991).
[17] G. Taylor, Proc. R. Soc. London, Ser. A **313**, 453 (1969).
[18] X. D. Sci, Michael P. Brenner, and Sidney R. Nagel, Science **265**, 219 (1994).
[19] A. Renau, F. H. Read, and J. K. Brunt, J. Phys. E **15**, 453 (1982).
[20] J. A. Tsamopoulos, T. R. Akylas, and R. A. Brown, Proc. R. Soc. London, Ser. A **401**, 67 (1985).
[21] O. A. Basaran and L. E. Scriven, Phys. Fluids A **1**, 795 (1989).
[22] V. E. Badan, V. V. Vladimirov, V. N. Gorshkov, and I. A. Soloshenko, Zh. Tekh. Fiz. **63**(6), 47 (1993) [Tech. Phys. **38**, 457 (1993)].
[23] R. Natarajan and R. A. Brown, Proc. R. Soc. London, Ser. A **410**, 209 (1987).
[24] G. Taylor, Proc. R. Soc. London, Ser. A **280**, 383 (1964).
[25] O. A. Basaran and L. E. Scriven, Phys. Fluids A **1**, 799 (1989).

Translated by D. H. McNeill